ADVANCED MATERIALS

Supporting Information

for *Adv. Mater.*, DOI: 10.1002/adma.201301472

Reconfigurable Infrared Camouflage Coatings from a Cephalopod Protein

*Long Phan, Ward G. Walkup IV, David D. Ordinario, Emil Karshalev, Jonah-Micah Jocson, Anthony M. Burke, and Alon A. Gorodetsky**

Submitted to ADVANCED MATERIALS

Supporting Information

DOI: 10.1002/adma.201301472

Reconfigurable Infrared Camouflage Coatings from a Cephalopod Protein

By *Long Phan*, *Ward G. Walkup IV*, *David D. Ordinario*, *Emil Karshalev*, *Jonah-Micah Jocson*, *Anthony M. Burke*, and *Alon A. Gorodetsky**

Alon A. Gorodetsky,* Long Phan, David D. Ordinario, Emil Karshalev, Jonah-Micah Jocson, Anthony M. Burke
Department of Chemical Engineering and Materials Science
University of California, Irvine
Irvine, CA 92697 (USA)
E-mail: (alon.gorodetsky@uci.edu)

Ward G. Walkup IV
Division of Biology
California Institute of Technology
Pasadena, CA 91125 (USA)

Detailed Description of Film Thickness Calculations. The theoretical film thicknesses were calculated based on thin-film interference theory.[1] At normal incidence, the reflected light obeys the formula:

$$m * \lambda = 2 * n * d$$

where *m* is an integer that describes wavelength order, λ is the peak reflected wavelength, *n* is the refractive index of the film, and *d* is the film thickness. At non-normal incidence, a factor of $\cos(\theta_F)$ must be introduced, where θ_F is the angle in the film that can be calculated with Snell's Law. The formula above is applicable for measurements performed with an integrating sphere accessory because the angle of incidence for the integrating sphere is less than 10° from normal incidence, leading to a small deviation in the theoretical thickness (< 4 %).[1] The graphene oxide adhesion layer used in our experiments was very thin with a high refractive index, so it did not dramatically influence the calculated values. The refractive indices used for the calculations were measured at Filmetrics (San Diego, CA) using a Filmetrics F20-UV spectrometer (Figure S13).

Surface Treatment. The APTES/graphene oxide surface treatment yielded smooth RfA1 films over large areas. Alternative surface functionalization schemes, such as triethoxyoctylsilane (OTES) treatment, UV-Ozone exposure, and APTES treatment without graphene oxide, produced less reliable results.

Response of Reflectin Films to Chemical Stimuli. We screened numerous potential solvents for shifting the reflectance of RfA1 coatings. These solvents included acetic acid, ethanol, ethyl acetate, isopropanol, triethyl amine, dimethyl formamide, and dimethyl sulfoxide. Such stimuli produced small spectral shifts, with the exception of acetic acid vapor.

[1] A. Lipson, S. G. Lipson, H. Lipson, *Optical Physics*, 4th ed., Cambridge University Press, Cambridge, **2010**.

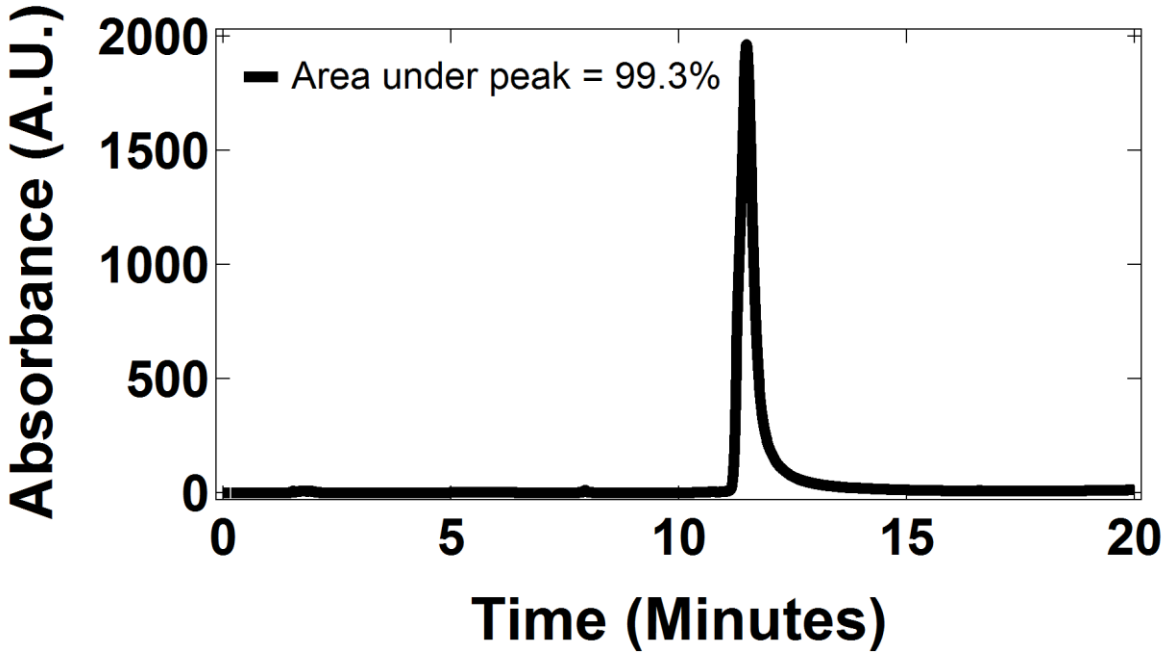

Figure S1. Typical reverse phase HPLC chromatogram of RfA1 following immobilized metal affinity chromatography. The presence of a single peak, whose area integrates to > 99 % of the total peak area represented in the chromatogram, indicates the excellent purity of our protein. The single peak also indicates that higher order aggregates are not present during chromatographic purification. RfA1 was eluted in a gradient evolved from 5 % Buffer A:95 % Buffer B to 95 % Buffer A:5 % Buffer B at a flow rate of 0.5 mL min^{-1} over 20 minutes (Buffer A: 99.9 % H_2O, 0.1% TFA; Buffer B: 95 % acetonitile, 4.9 % H_2O, 0.1% TFA).

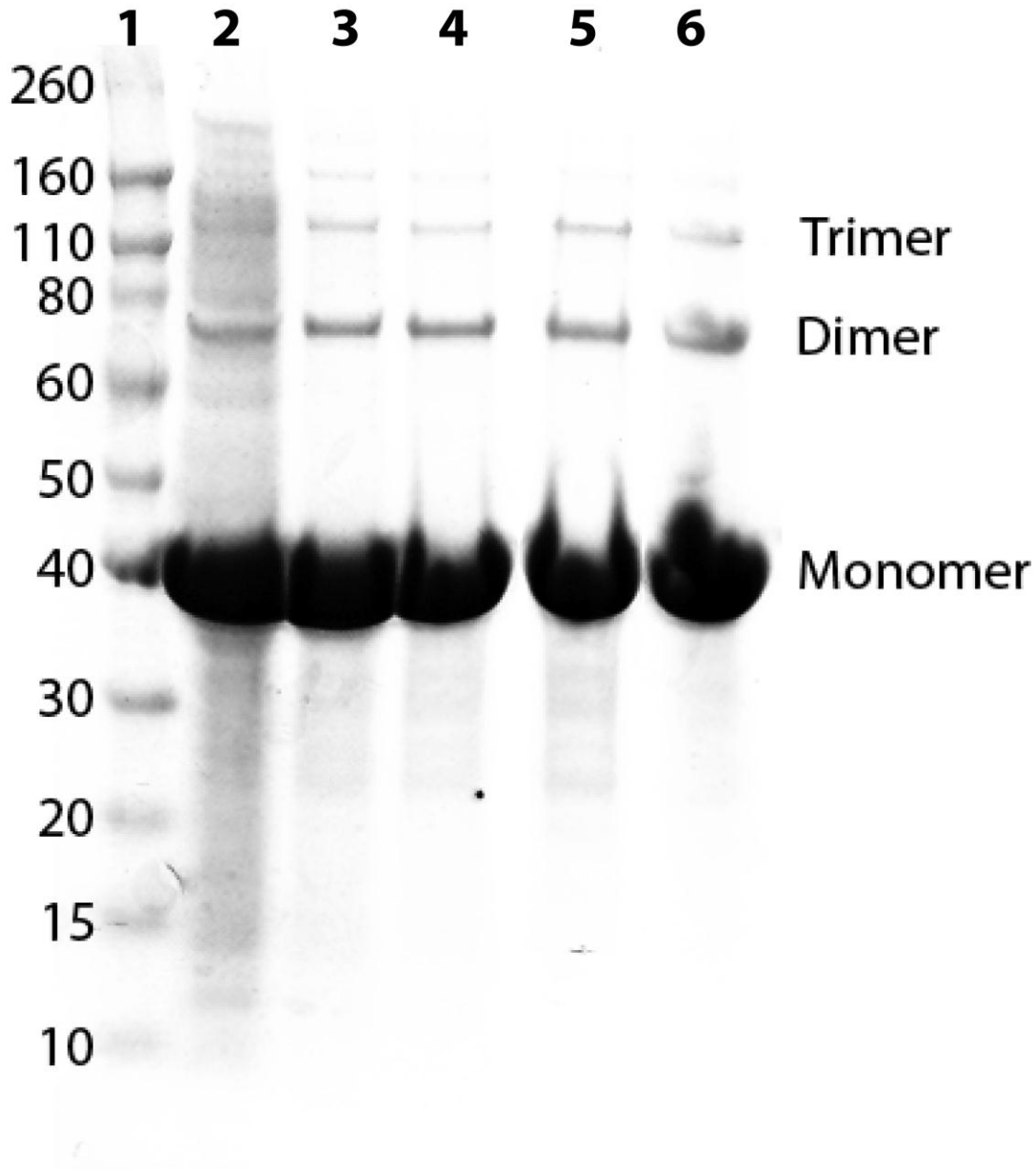

Figure S2. Analysis of the purification of RfA1 *via* denaturing gel electrophoresis. Samples of RfA1 at different stages of the purification process were analyzed by SDS-PAGE and visualized by GelCode Blue Stain Reagent (Thermo Scientific). Lane 1: Novagen Sharp protein ladder for molecular weights of 10 kDa to 260 kDa. Lane 2: Total protein fraction after cell pellet resuspension and lysis. Lane 3: Insoluble protein fraction following centrifugation. Lane 4: Inclusion body fraction after resuspension in denaturing buffer. Lane 5: Eluate from the IMAC (HisPur Cobalt Resin) gravity column. Lane 6: Eluate from C18 reverse phase HPLC column. Bands corresponding to monomeric (44,605 Da) and oligomeric RfA1 are labeled accordingly.

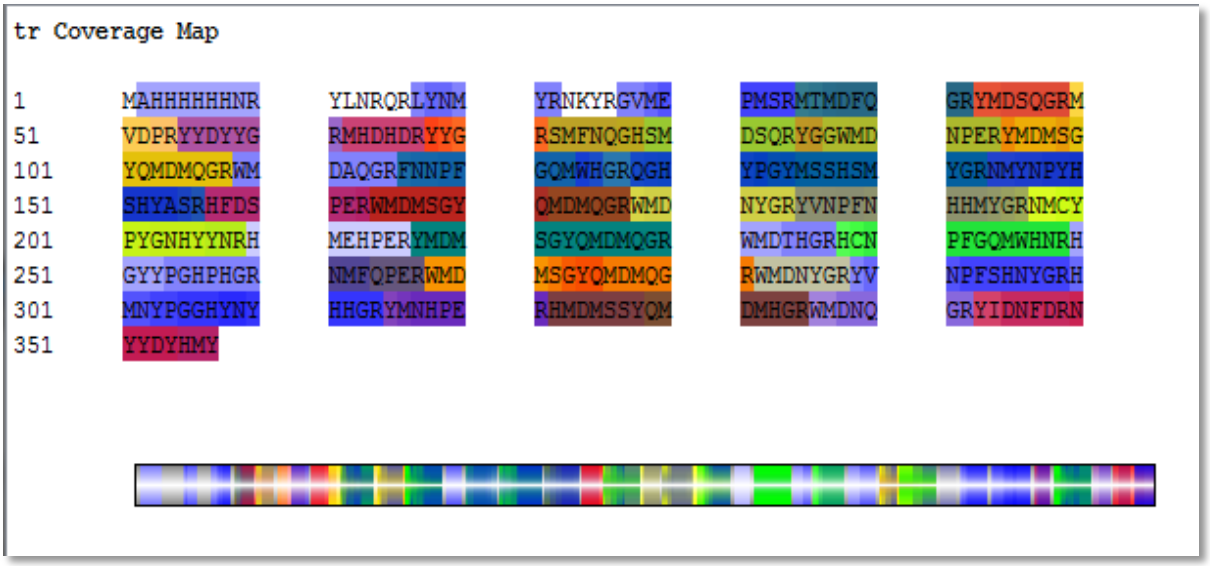

Figure S3. Peptide coverage map of RfA1 protein sequence produced by in-gel digestion of purified soluble RfA1 with porcine trypsin. The color coding corresponds to different tryptic peptide fragments. Sequence coverage exceeded 96%, definitively confirming the purified protein's identity as RfA1.

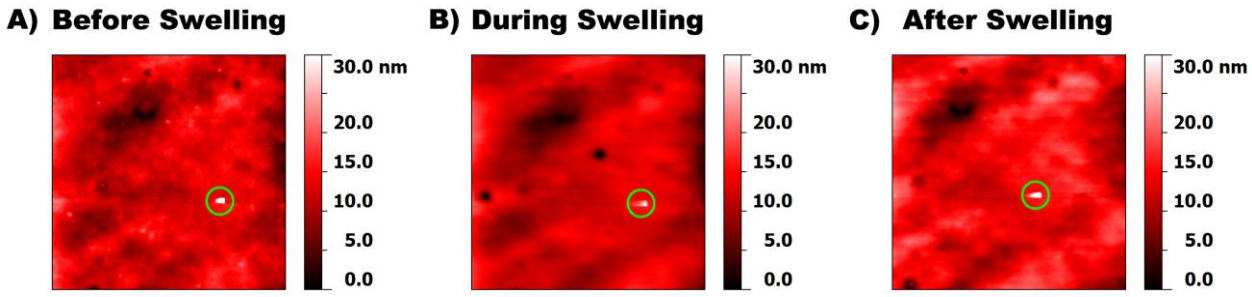

Figure S4. A) Atomic force microscopy (AFM) images of a RfA1 film A) before, B) during, and C) after exposure to acetic acid vapor. The film morphology does not exhibit any signs of degradation during and after the incubation. Note that the AFM images represent the same spot on each film as demonstrated by the green marker.

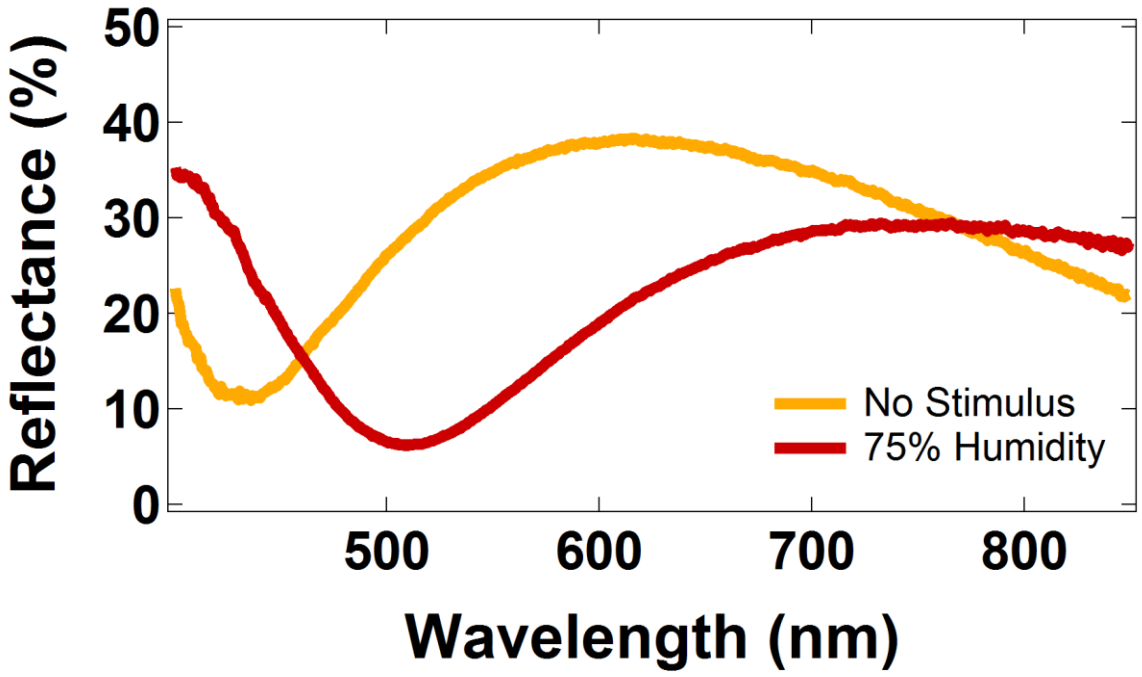

Figure S5. Reflectance spectra of an RfA1 orange film before (orange curve) and after (red curve) exposure to water vapor (relative humidity of 75%).

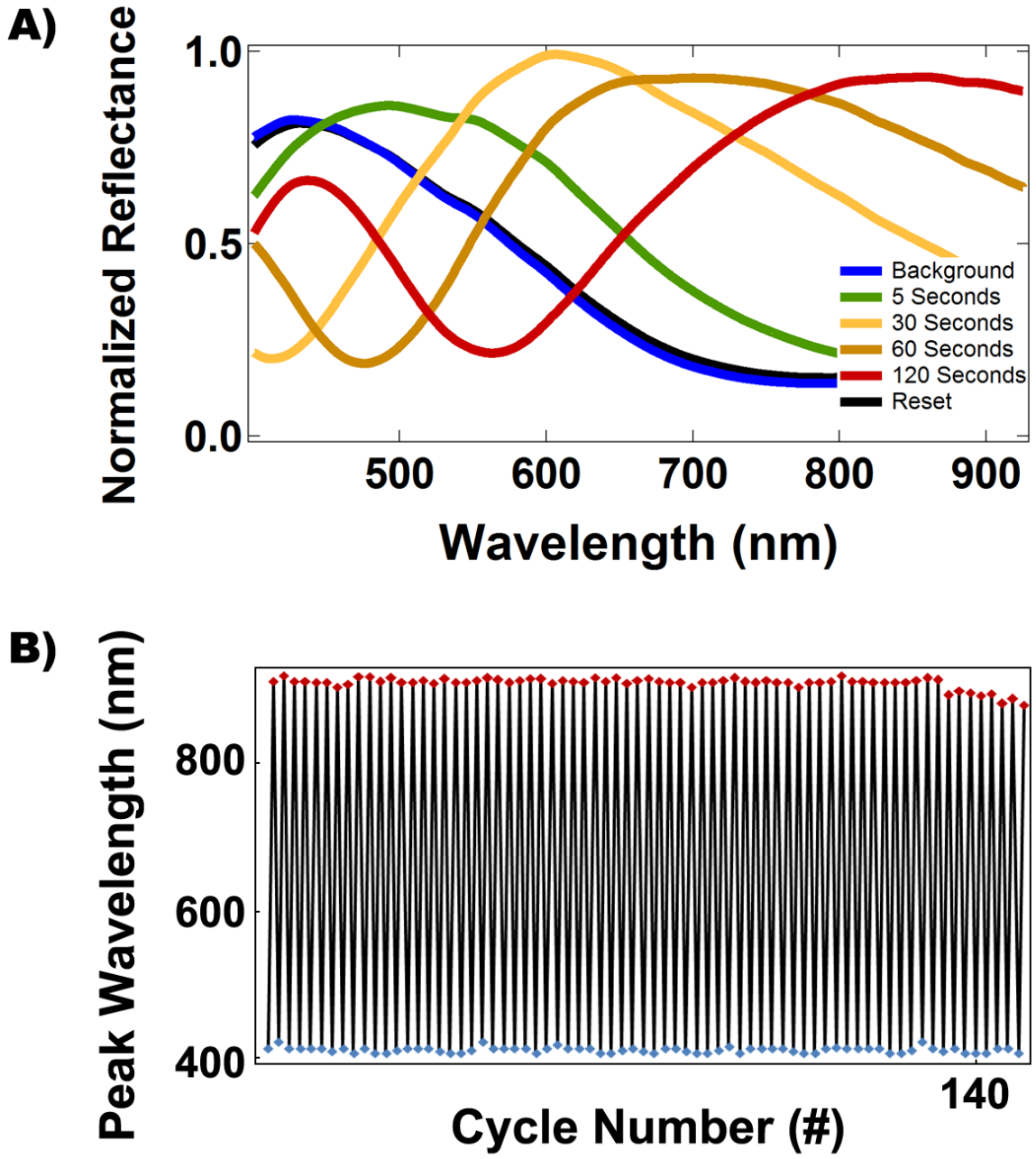

Figure S6. A) Change in the reflectance for an RfA1 film as a function of time following application of acetic acid vapor. The spectra were collected with a bare fused silica substrate as the standard and normalized with respect to the maximum reflectance value. Note that the initial reflectance spectra can be recovered within seconds by a "reset" or removal of the acetic acid vapor stimulus (the blue and black traces overlap). B) Illustration of reversible cycling of the RfA1 films between a peak reflectance of λ = 400 nm in the visible (blue markers) and a peak reflectance of λ = 900 nm in the infrared (red markers). The cycling was performed by exposure to solvent vapor from a glacial acetic acid solution. The experiment was repeated until the film demonstrated a degradation in the reflectance intensity.

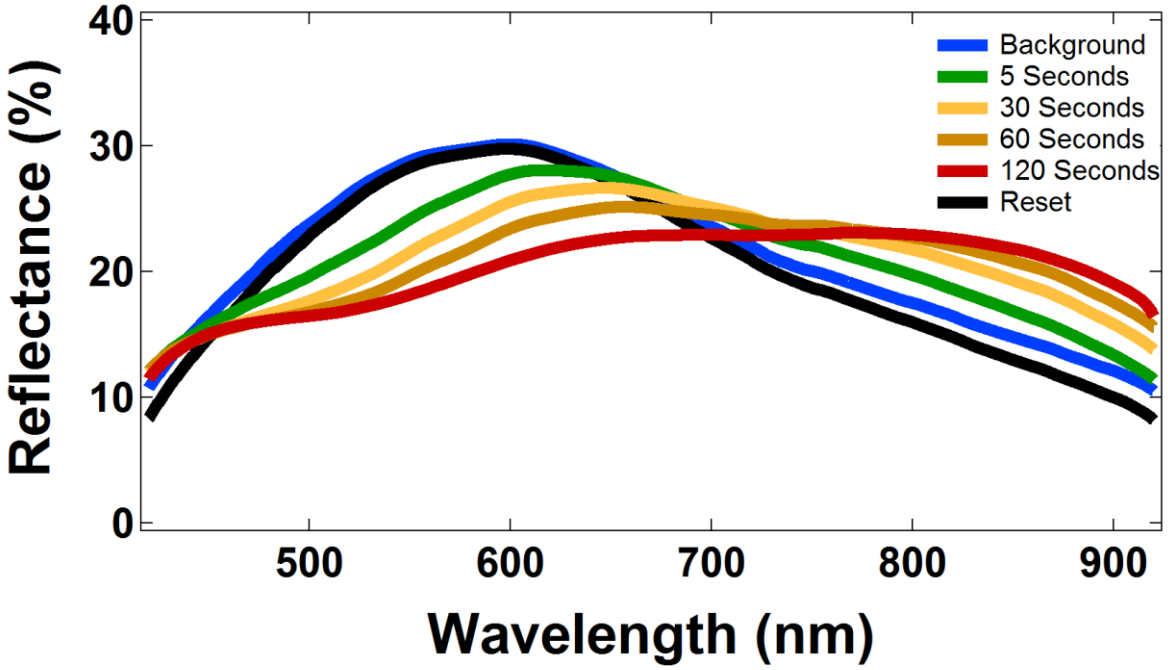

Figure S7. Reflectance spectra for a Bovine Serum Albumin (BSA) film as a function of time following application of acetic acid vapor. The film preparation and treatment were identical to those used for RfA1 films. The curves have been smoothed for clarity. Note the small peak shift.

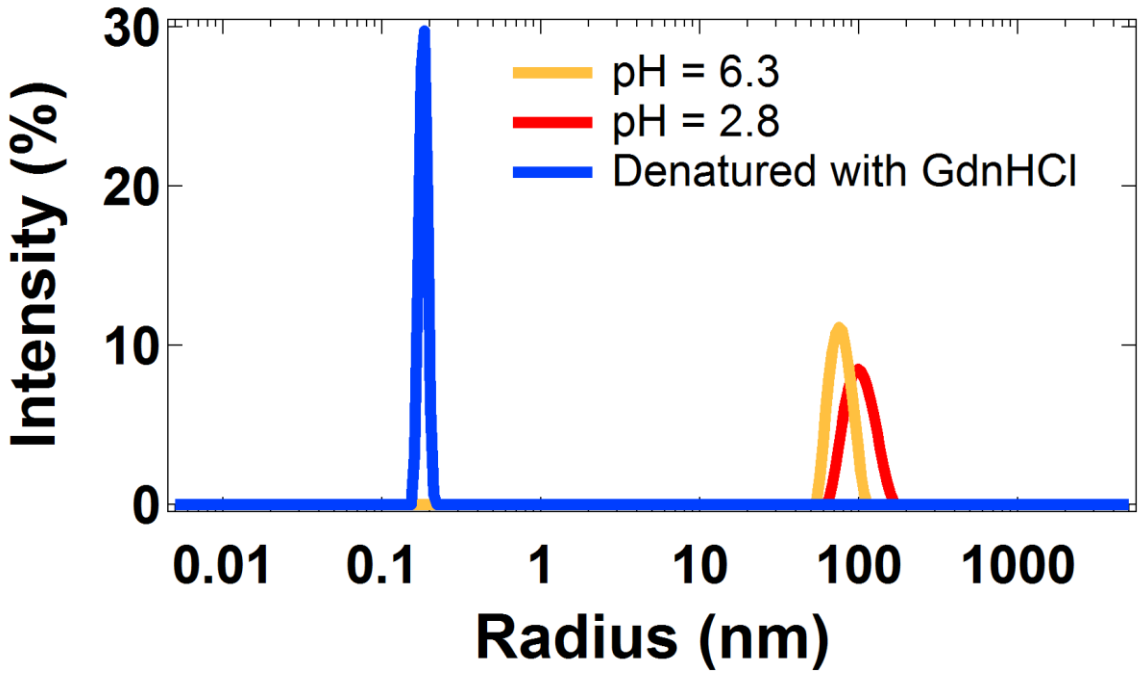

Figure S8. Dynamic light scattering spectra for RfA1 (0.5 mg/mL) at pH 6.3 (orange curve) and pH 2.8 (red curve). The measured R_H value increases from 75 (±11) nm at pH 6.3 to 99 (±14) nm at pH 2.8. The size of the aggregated RfA1 is distinct from that reported in reference 15 in the text, presumably due to differences in the protein and salt concentrations. The aggregation of RfA1 was confirmed by the introduction of guanidinium hydrochloride (GdnHCl) into the solution, which denatured RfA1 (blue curve), yielding an R_H value of < 1 nm.

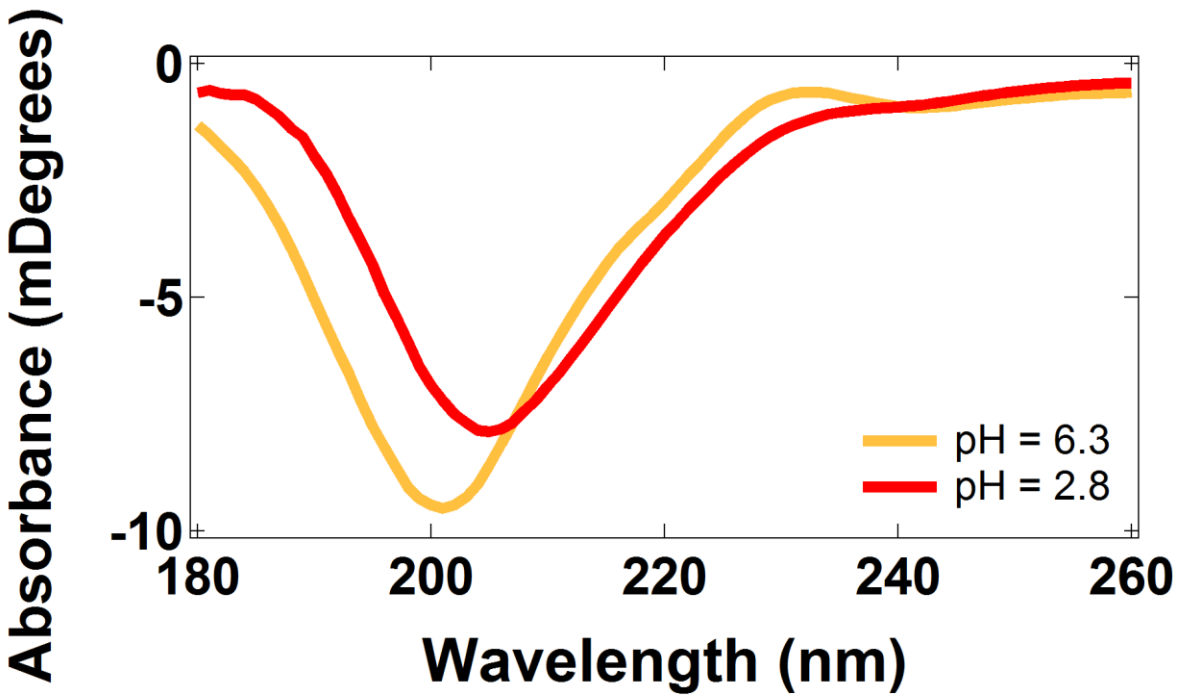

Figure S9. Circular dichroism spectra for RfA1 (~0.5 mg/mL) at pH 6.3 (orange curve) and pH 2.8 (red curve). The spectra were analyzed with DICHROWEB software (http://dichroweb.cryst.bbk.ac.uk), indicating that RfA1 possesses little to no alpha helical or beta strand secondary structure, which is in excellent agreement with previous findings (see references 13 to 17 in the text).

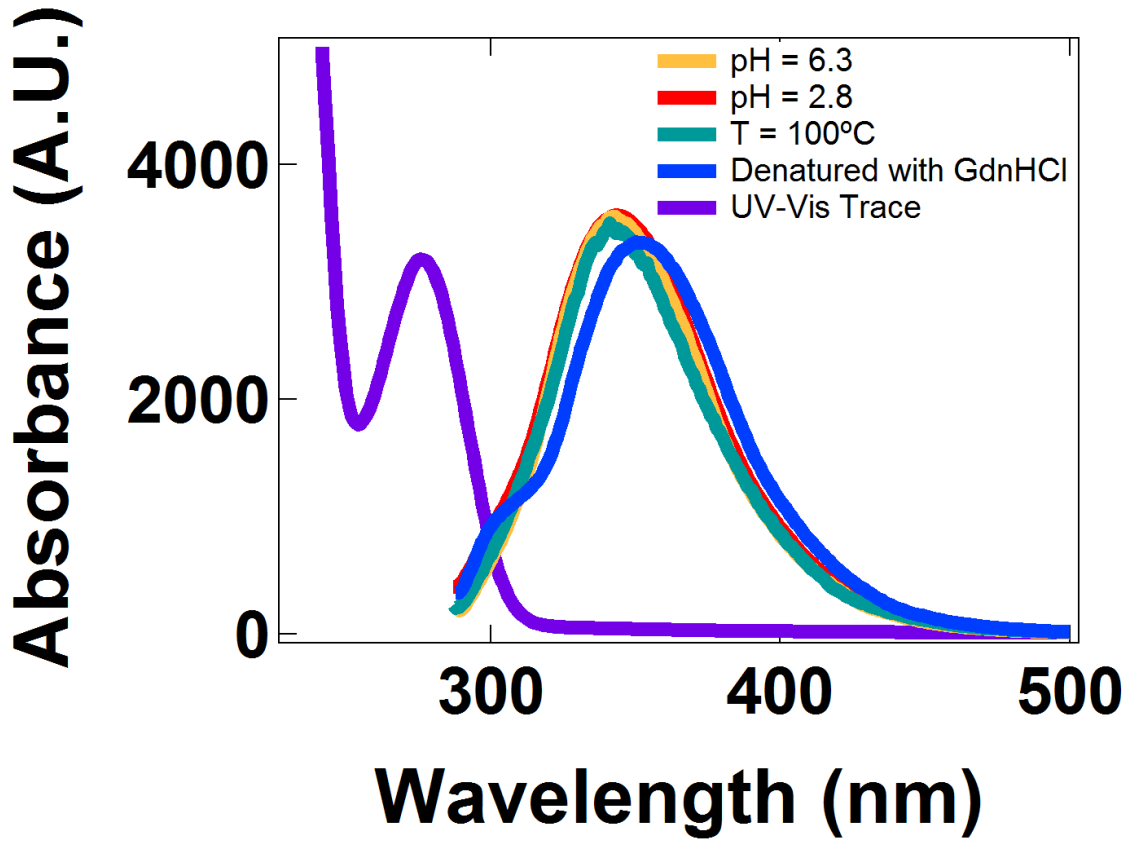

Figure S10. Fluorescence and UV-visible absorbance spectra for RfA1 (0.5 mg/mL). The absorbance spectrum (purple curve) displays a characteristic peak at λ = ~ 280 nm. The fluorescence spectra were obtained for RfA1 (0.5 mg/mL) at pH 6.3 (orange curve), pH 2.8 (red curve), and at a temperature of 100°C (green curve) (excitation wavelength of λ = 282 nm). There is virtually no change in the fluorescence spectra with a change in pH (red curve) or temperature (green curve), indicating RfA1 maintains its conformation. However, upon addition of GdnHCl (blue curve), the fluorescence spectrum maxima shifts to λ = ~ 347 nm and a new peak appears at λ = ~ 300 nm. Absorbance at λ = ~ 300 nm is characteristic of solution exposed tyrosine residues, i. e. RfA1 denaturation.

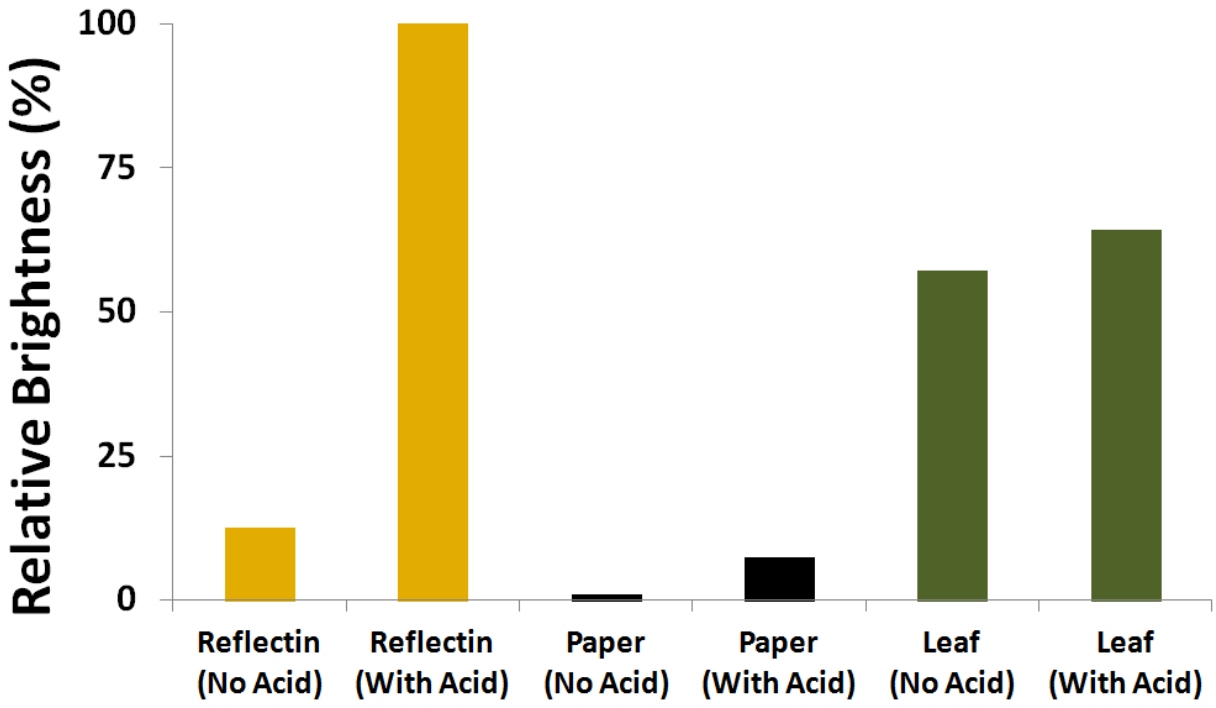

Figure S11. Integrated infrared brightness values measured for an RfA1 film, a piece of paper, and a *Buxus* plant leaf in the presence and absence of acetic acid vapor. The values were extracted by analyzing Figure 3B in the main text and normalized to the maximum brightness.

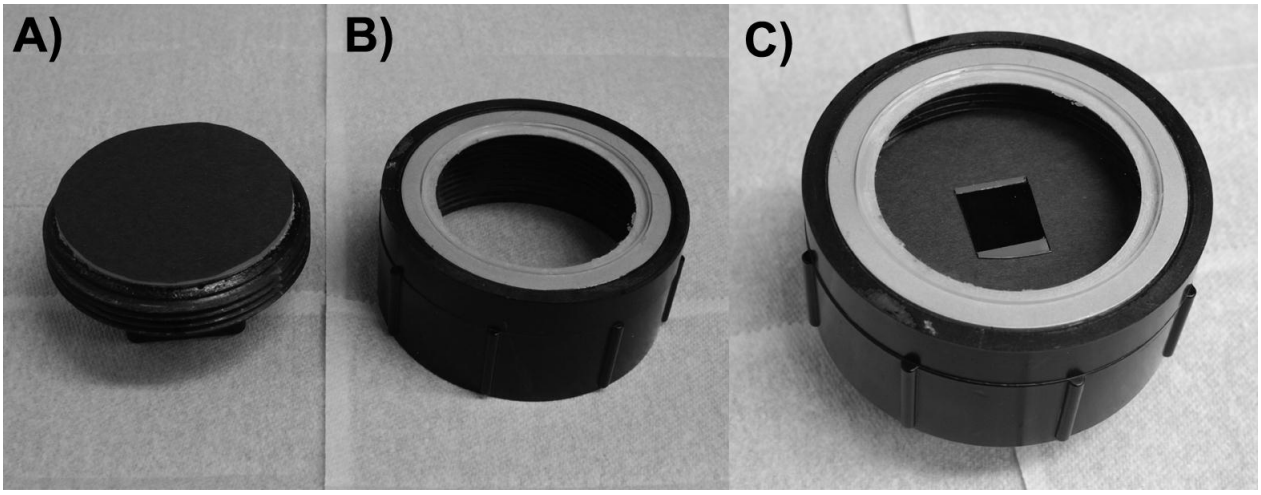

Figure S12: Pictures of the housing used for exposure of the RfA1 coated substrates to acetic acid vapor. A) The bottom part of housing. B) The top part of housing. C) The integrated housing containing an RfA1 coated substrate.

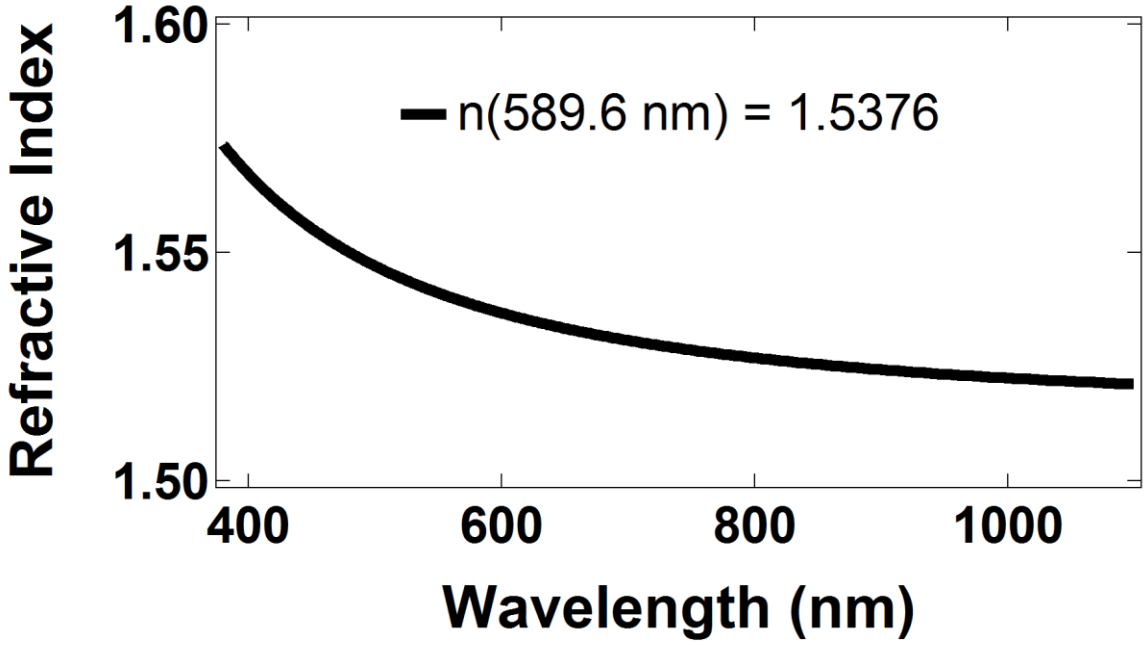

Figure S13. The refractive index of the RfA1 films measured at Filmetrics (San Diego, CA) using a Filmetrics F20-UV spectrometer with a deuterium and tungsten-halogen white light source (effective wavelength range of λ = 200 nm to λ = 1100 nm). The refractive index was measured at λ = 632.8 nm with a resolution less than 1 nm. The data was acquired normal to the substrate surface.